Closing the gap from spatio-temporal displacement monitoring to geomechanical process understanding of cascading multi-hazards caused by deep-seated gravitational slope deformations

Johannes Branke, Barbara Schneider-Muntau
Department of Infrastructure, Geotechnical Engineering Unit, Universität Innsbruck, Innsbruck, Austria

Jan Pfeiffer, Margreth Keiler
Institute for Interdisciplinary Mountain Research, Austrian Academy of Sciences, Innsbruck, Austria

Thomas Zieher
Institute for Natural Hazards, Austrian Research Centre for Forests (BFW), Innsbruck, Austria

Martin Rutzinger, Magnus Bremer, Margreth Keiler
Institute of Geography, Universität Innsbruck, Innsbruck, Austria

Bernhard Gems
Department of Infrastructure, Hydraulic Engineering Unit, Universität Innsbruck, Innsbruck, Austria

ABSTRACT: Active deep-seated gravitational slope deformations (DSGSDs) and interlinked secondary processes such as rockfalls and debris flows pose multiple threats to livelihoods in mountain regions. A currently active part (~0.35 km^2) of the Reissenschuh DSGSD (Schmirn valley, Tyrol, Austria) shows considerable displacement rates of about 1 m per year. This remarkable relocation of material constantly changes the topography and leads to a pronounced activity of debris flow and rockfall at the landslide toe. This contribution focuses on understanding the interactions of DSGSD activity (rock mass supply) and interlinked cascade dynamics to assess their complex triggering mechanisms and related secondary processes. It gives an overview of previous and ongoing monitoring campaigns and presents preliminary findings on cascade process interactions.

Keywords: Natural hazard research, deep-seated gravitational slope deformation, cascade multi-hazard, landslide.

1 INTRODUCTION

Deep-seated gravitational slope deformations (DSGSDs) are a widespread phenomenon in mountainous regions (Crosta et al. 2013). They typically consist of slow-moving nested slope failures featuring complex deformation patterns that can be recognized by conspicuous surface features (Agliardi et al. 2012). Secondary slope instabilities (e.g., deep-seated rock slides) are common at their bulged foot. They are characterized by enhanced activity and pose a certain probability to accelerate and transform to large catastrophic slope failures (Fukuzono 1985, Ostermann and Sanders 2017). Moreover, pronounced displacement rates infer a constant rock mass supply preconditioning the occurrence of debris flow and rock fall events. Such process inter-dependencies pose multi-hazard-cascades potentially harming infrastructure or society (Mergili et al. 2020, Cicoira et al. 2022). Investigations and a precise understanding of multi-hazard cascades and geomorphic feedback originating from active deep-seated landslides are essential and yet not fully explored (Korup et al. 2010). Moreover, the representation of such complex processes in numerical models is challenging but key for process understanding and mitigation (Crosta et al. 2017). This contribution identifies, presents and compiles essential monitoring data that is required to describe multi-hazards originating from the Reissenschuh deep-seated landslide situated in the Schmirn valley (Tyrol, Austria). Geodetic and remote sensing measurements are performed for analyzing landslide kinematics in space and time. Surface displacements and volumes of mass relocation are quantified based on periodic measurements with a Differential Global Navigation Satellite System (DGNSS), by Terrestrial, Airborne and Uncrewed aerial vehicle-based Laser Scanning (TLS, ALS, ULS) and historical aerial image photogrammetry (PHG). Parameters characterizing the recent debris flows at the foot slope are assessed by line counting and volume sampling of the debris flows material. Integrating the resulting manifold data sets aims at answering the following research questions:

- Which monitoring variables are essential and required to describe and quantify complex process cascades originating from a slow-moving deep-seated rock slide?
- Which process cascade(s) can be observed, described and quantified by existing data?
- Which data and model applications are yet missing to give a holistic picture of prevailing process cascades?

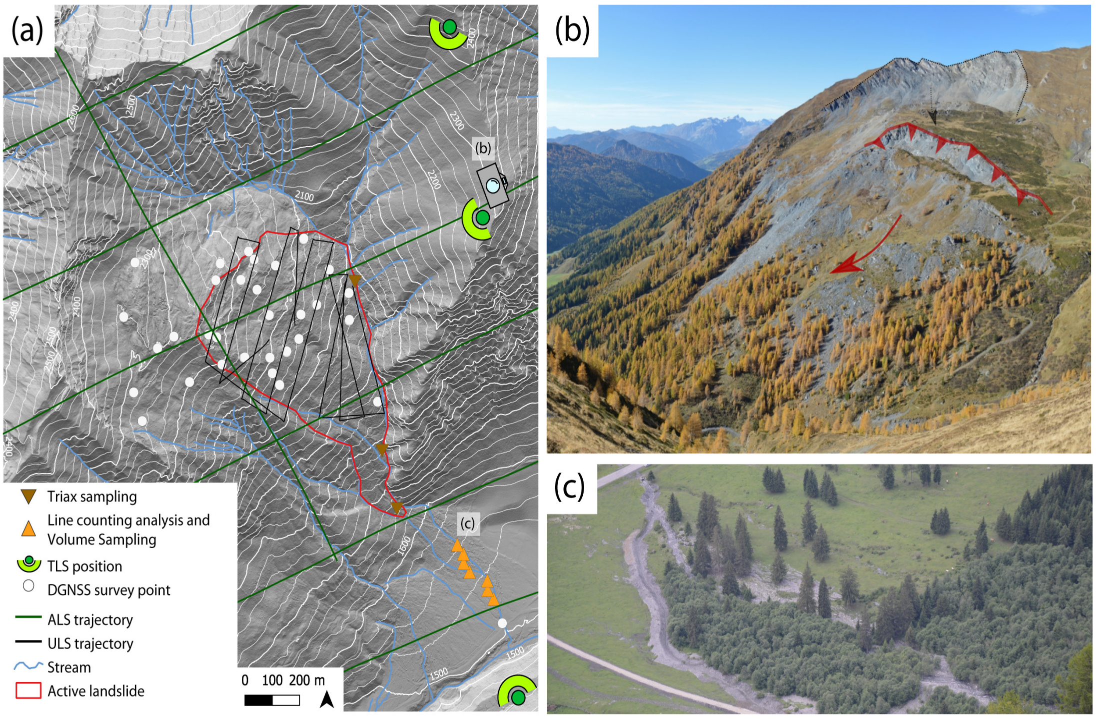

Figure 1. Overview of the study site with marked locations of measurement setup shown in (a). (b) Photograph of Reissenschuh landslide towards west (J. Branke, 23.10.19) with sketched paleo-movement (black dotted), active rock slide part (red) and movement direction (arrow). (c) shows the debris flow channels adjacent to the landslide toe towards the road (J. Branke 30.06.22).

2 STUDY AREA

The Reissenschuh landslide (deep-seated rock slide; classification after Cruden & Varnes 1996) is located in the Schmirn valley (Tyrol, Austria) on a south-east exposed slope. Based on multi-temporal TLS, ULS and ALS acquisitions, an active part moving at considerable rates of over 1 m per year was identified between 1650 m a.s.l. and 2200 m a.s.l. (Pfeiffer et al. 2018, 2019). It is surrounded by a ridge and summits reaching 2600 m a.s.l. Penninic Bündner schists (i.e., Mica-calcareous phyllite overlaying graphite phyllite) represent the lithological predisposition of observable large slope instabilities (Rockenschaub et al. 2003). The mean schistosity of the landslide surrounding rocks dips with 25° towards north (344°). The active landslide area initiates at the lower eastern part of a large fossil landslide deposit and covers an area of 0.35 km^2. It has a funnel-shaped geometry whereas the width is largest (approx. 500 m) at the scarp between 2100 and 2200 m a.s.l.

and lowest at the tongue-shaped toe (approx. 50 m) at 1650 m a.s.l. (Figure 1a, b). The active landslide is located within an approximately 2 km^2 large torrential catchment.

Secondary natural hazard processes such as debris flows occurred on a regular basis in the past. As Wei et al. (2018) point out, the combination of sufficient loose solid materials, water runoff and steep terrain are necessary causes and triggers. In the present case, steep terrain and a sufficient loose solid material are available and assumed to be constantly reproduced by the deep-seated and active landslide inferring significant rock mass degradation (e.g., weakening and fracturing). Occasionally occurring heavy precipitation events then provide the last ingredient to trigger debris flows at the catchment around the Reissenschuh landslide (Figure 1c).

In addition, the activity of the deep-seated landslide is assumed to be influenced by precipitation events inferring increased pore-pressure conditions expressed by accelerated movements. Rock slide activity and debris flows can occur simultaneously and likely influence each other. Debris flows initiating at the active deep-seated rock slide were observed to reach long run outs affecting the federal road by blockage of the outlet below the road. In a further scenario the debris could dam the valley river, potentially leading to a severe flooding event harming upstream settlements.

3 MATERIALS AND METHODS

Kinematic monitoring of the landslide consists of geodetic and remote sensing-based measurements at single points and area-wide. Periodic DGNSS measurements are performed since 2016 at 47 distributed measurement points (Figure 1a). Area-wide and three-dimensional displacement time series were reconstructed from historical PHG between 1954 and 2019 (1971/73, 2007, 2010), annual TLS from different scanning positions as indicated in Figure 1a since 2016 and ULS since 2018. Point clouds derived from overlapping aerial photographs by photogrammetry i.e., Structure from Motion (SfM), or from laser scanning were classified into ground and non-ground points using the Triangulated Irregular Network densification algorithm proposed by Axelsson (2000). Digital Terrain Models (DTM) representing the bare Earth surface excluding vegetation were used to assess multi-temporal surface changes. Volume changes between consecutive DTMs were assessed by raster differencing. 2.5D displacement vectors were derived using the IMage CORRelation (IMCORR) algorithm implemented in the open-source software SAGA GIS (Conrad et al. 2015, Bremer 2012). Shaded relief images derived from the DTMs were used as input to infer correspondences between raster cells. In addition to the algorithm proposed by Fahnestock et al (1992), the applied and modified version of IMCORR is capable to additionally consider the DTMs' elevation information to determine 2.5D displacements (Bremer 2012, Pfeiffer et al. 2018). On the debris flow cone Line Count Analysis (LCA) and Volume Samples (VS) were conducted to characterize the grain size distribution of recent debris flows (Figure 1a). At recent erosional areas in vicinity of the stream, where the landslide collides with the opposite slope, samples of the sliding mass were taken for further triaxial shear tests to quantify parameters for the replication of the landslide behavior with numerical models.

4 RESULTS

4.1 Landslide surface deformation and process interaction

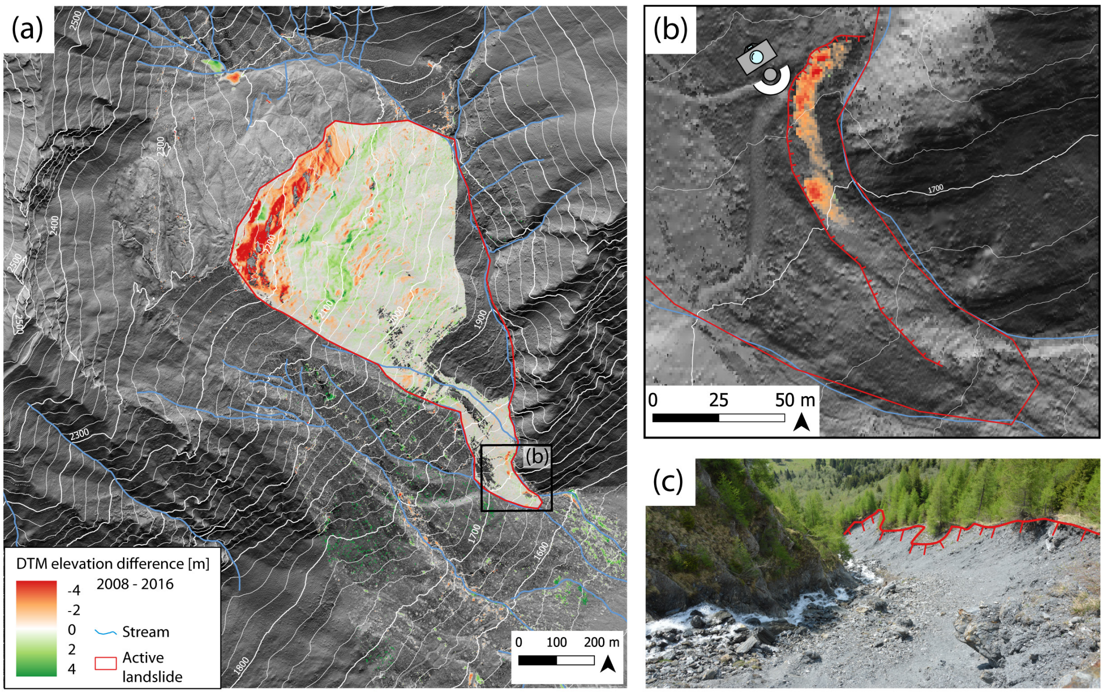

Figure 2. (a) Map of elevation differences between ALS 2008 and TLS 2016 DTM; (b) detail of map shown in (a) indicating significant torrential erosion of approx. 975 m^3 at the active landslide's toe; (c) photograph by J. Branke taken 16.05.2022 from a position shown in (b) and showing embankment erosion, red line indicating the scarp.

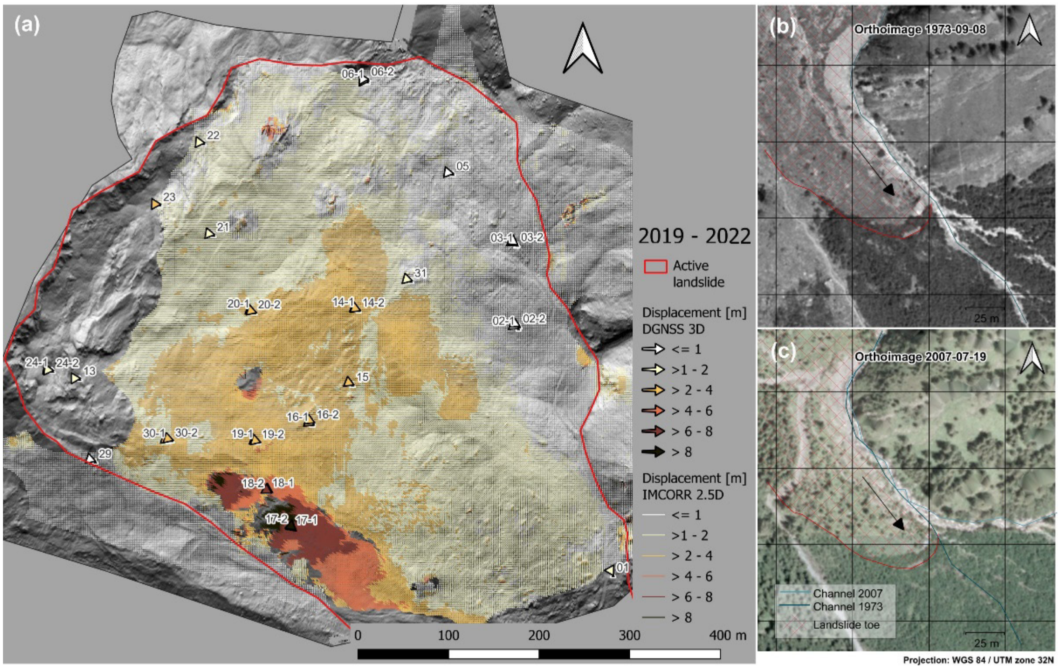

Figure 3. Displacement map of image correlation (IMCORR) and differential global navigation satellite system (DGNSS) results for the time interval mid-2019 to mid-2022 (a); Maps showing the location of the landslide toe mapped from orthoimageries 1973-09-08 (b) and 2007-07-19 (c) and respective elevation models. An advance of 5.5 m is recognizable and assumed to redirect the stream and path of debris flows. The grid spacing is 50 m in the coordinate system of EPSG:32632.

Regarding the spatial movement patterns on the Reissenschuh landslide, noticeable differences are observable. Besides of the considerable landslide deformation characterized by spatio-temporal varying displacements, some topographic changes observable on the active landslide and in the vicinity of the torrential stream are related to secondary mass relocation processes. Examining the map of elevation differences between DTMs derived from ALS in 2008 and TLS in 2016 (Figure 2a), an area of significant denudation is apparent at 1700-1750 m a.s.l. (Figure 2b). Whereas overall negative elevation differences right below the scarp of the active landslide at 2200 m a.s.l. are clearly attributed to the prevailing landslide-induced subsidence, the negative elevation differences along the embankment of the stream (1700-1750 m a.s.l.) at the eastern landslide margin are likely associated to fluvial or torrential erosion causing secondary and spontaneous slope failures (Figure 2c). During the observation period of 8 years, a volume of 975 m^3 was relocated from the embankment into the stream and transported further by debris flows.

Rasterized ULS point clouds processed by IMCORR enable an area-wide visualization of movement patterns. Comparing ULS campaigns (Bremer et al. 2019) 2019 to 2022 pronounced movements (3-8 m) on a debris field situated at the south-western landslide margin are visible. The movement direction and the movement magnitude are in agreement with the DGNSS measurements conducted at survey points on boulders in the active landslide body (detailed description of the measurement setup see Pfeiffer et al. 2018). During the three-year time interval, single areas did show displacements up to 8 m in total (Figure 3a).

At the landslide toe (around 1650 m a.s.l.), indenting with a debris flow cone which leads to the Schmirnbach at 1490 m a.s.l. historical aerial imagery and resulting photogrammetric 3D point clouds show that the channel was relocated towards north on the debris flow cone (Figure 3b, c) between 1973 and 2007. Furthermore, the mapped landslide toe has advanced by 5.5 m in that period. This movement and the respective change of the topography may have redirected the stream on the debris flow cone. Accordingly, the analysis of historical imagery indicates the influence of the advancing deep-seated rock slide on the flow paths of episodic debris flows.

4.2 Geotechnical characteristics of debris flow and debris slide material

For further assessment of cascading processes, the previously described inter-linkage with debris flows is of special interest. The lower bound values resulting from three laboratory triaxial shear tests show a mean internal friction angle around 32° and values for cohesion vary between 10 and 25 kPa. For the debris cone LCAs and VSs are in good agreement. The results show a low share of fine-grained particles (< 4 mm), which are assumed to be washed out. In comparison with upstream VS, the VS on the debris flow cone show a larger share of larger grain sizes (> 63 mm), which is due to the small slope angle and therefore common to deposit areas. This data will be used in further investigations of numerical debris flow run-out calculations.

5 CONCLUSIONS

We identified, presented and compiled essential monitoring data that is required to describe multi-hazards originating from the Reissenschuh landslide situated in Tyrol, Austria. With the help of extensive surface monitoring, displacements and movement patterns can be analyzed in space and time. Areas of increased (up to 8 m in three years) displacement were highlighted. Interaction of the active rock and debris slide toe with the stream was presented. It was shown that on the one hand the fluvial or torrential erosion of the active debris slide material caused secondary slope failures and supplied material for debris flows. On the other hand, the advance of the active slide toe very likely influenced and changed the flow path of the stream and the run-out zone of debris flows. Future investigations will focus on the replication of the process cascade by geomechanical modeling of the active slide combined with numerical run-out simulations of interlinked debris flow events. Thereby, presented and assessed data and variables including landslide deformation, volume of mass relocation as well as determined material characteristics from LCAs, VSs and shear-tests are crucial components for appropriate model parametrization.

ACKNOWLEDGEMENTS

Funding was received from the Universität Innsbruck in support of the Innsbruck Doctoral College "Natural Hazards in Mountain Regions" (https://www.uibk.ac.at/alpinerraum/idcs/dp-mountainhazards/).

REFERENCES

Agliardi, F., Crosta, G. B., & Frattini, P. (2012). Slow rock-slope deformation. In J. J. Clague & D. Stead (Eds.), Landslides (1st ed., pp. 207–221). Cambridge University Press. DOI: 10.1017/CBO9780511740367.019

Axelsson, P. (2000). DEM generation from laser scanner data using adaptive TIN models. ISPRS- International Archives of the Photogrammetry, Remote Sensing and Spatial Information Sciences, 33, 110–117.

Bremer, M. (2012). IMCORR—Feature Tracking. [SAGA-GIS Tool Library Documentation (v8.4.0)] https://saga-gis.sourceforge.io/saga_tool_doc/8.4.0/grid_analysis_19.html [last accessed: 20.02.2023].

Bremer, M., Zieher, T., Pfeiffer, J., Petrini-Monteferri, F., & Wichmann, V. (2019). Monitoring der Großhangbewegung Reissenschuh (Schmirntal, Tirol) mit TLS und UAV-basiertem Laserscanning. 20. Internationale Geodätische Woche Obergurgl 2019., 321–330.

Cicoira, A., Blatny, L., Li, X., Trottet, B., & Gaume, J. (2022). Towards a predictive multi-phase model for alpine mass movements and process cascades. Engineering Geology, 310, 106866. DOI: 10.1016/j.enggeo.2022.106866

Conrad, O., Bechtel, B., Bock, M., Dietrich, H., Fischer, E., Gerlitz, L., Wehberg, J., Wichmann, V., & Böhner, J. (2015). System for Automated Geoscientific Analyses (SAGA) v. 2.1.4. Geoscientific Model Development, 8(7), 1991–2007. DOI: 10.5194/gmd-8-1991-2015

Crosta, G. B., Agliardi, F., Rivolta, C., Alberti, S., & Dei Cas, L. (2017). Long-term evolution and early warning strategies for complex rockslides by real-time monitoring. Landslides, 14(5), 1615–1632. DOI: 10.1007/s10346-017-0817-8

Crosta, G. B., Frattini, P., & Agliardi, F. (2013). Deep seated gravitational slope deformations in the European Alps. Tectonophysics, 605, 13–33. DOI: 10.1016/j.tecto.2013.04.028

Cruden, D. M., & Varnes, D. J. (1996). Landslide Types and Processes. In A. K. Turner & R. L. Schuster (Hrsg.), Landslides: Investigation and mitigation (S. 36–75). National Academy Press.

Fahnestock, M., Scambos, T. A., & Bindschadler, R. A. (1992). Semi-automated ice velocity determination from satellite imagery. Eos, Transactions American Geophysical Union, 73, 493.

Fukuzono, T. (1985). A new method for predicting the failure time of a slope. Proceedings of 4th International Conference and Field Workshop on Landslide., 1985, 145–150.

Korup, O., Densmore, A. L., & Schlunegger, F. (2010). The role of landslides in mountain range evolution. Geomorphology, 120(1–2), 77–90. DOI: 10.1016/j.geomorph.2009.09.017

Mergili, M., Jaboyedoff, M., Pullarello, J., & Pudasaini, S. P. (2020). Back calculation of the 2017 Piz Cengalo–Bondo landslide cascade with r.avaflow: What we can do and what we can learn. Natural Hazards and Earth System Sciences, 20(2), 505–520. DOI: 10.5194/nhess-20-505-2020

Ostermann, M., & Sanders, D. (2017). The Benner pass rock avalanche cluster suggests a close relation between long-term slope deformation (DSGSDs and translational rock slides) and catastrophic failure. Geomorphology, 289, 44–59. DOI: 10.1016/j.geomorph.2016.12.018

Pfeiffer, J., Zieher, T., Bremer, M., Wichmann, V., & Rutzinger, M. (2018). Derivation of Three-Dimensional Displacement Vectors from Multi-Temporal Long-Range Terrestrial Laser Scanning at the Reissenschuh Landslide (Tyrol, Austria). Remote Sensing, 10(11), 1688. DOI: 10.3390/rs10111688

Pfeiffer, J., Zieher, T., Rutzinger, M., Bremer, M., & Wichmann, V. (2019). Comparison and time series analysis of landslide displacement mapped by airborne, terrestrial and unmanned aerial vehicle based platforms. ISPRS Annals of Photogrammetry, Remote Sensing and Spatial Information Sciences, IV-2/W5, 421–428. DOI: 10.5194/isprs-annals-IV-2-W5-421-2019

Rockenschaub, M., Kolenprat, B., & Nowotny, A. (2003). 148 Brenner- Das westliche Tauernfenster. 7-38.

Wei, Z., Xu, Y.-P., Sun, H., Xie, W., & Wu, G. (2018). Predicting the occurrence of channelized debris flow by an integrated cascading model: A case study of a small debris flow-prone catchment in Zhejiang Province, China. Geomorphology, 308, 78–90. DOI: 10.1016/j.geomorph.2018.01.027